Journal of Petroleum and Gas Engineering Vol. 2(3), pp. 64-73, March 2011
Available online at http://www.academicjournals.org/JPGE
ISSN 2141-2677 ©2011 Academic Journals

Full Length Research Paper

Dehyrogenation catalysts of higher normal paraffins on a nanocrystalline γ-Al_2O_3 support: Different impregnation sequences

Mandana Akia[1,2,3]*, Seyed Mahdi Alavi[1], and Zi-Feng Yan[3]

[1]Chemical Engineering Department, Iran University of Science and Technology, Tehran, Iran.
[2]Chemical Engineering Department, Kermanshah University of Technology, Kermanshah, Iran.
[3]State Key Laboratory for Heavy Oil Processing, Key Laboratory of Catalysis, CNPC, China University of Petroleum, Dongying 257061, China.

Accepted date January 24, 2011

In this paper, high surface area nanocrystalline gamma alumina was synthesized by the sol-gel method using cationic surfactant. The Pt-based dehydrogenation catalysts consisting of promoters and support modifiers (Sn, In, Li and Fe) were prepared using the synthesized gamma alumina and employed in the dehydrogenation reaction of n-dodecane. The effects of different successive impregnation methods for Pt, Sn and In elements were investigated in dehydrogenation of normal dodecane. The prepared samples were characterized by X-ray diffraction (XRD), N_2 adsorption (BET), Scanning electron microscopy (SEM), Transmission electron microscopy (TEM) and Temperature programmed reduction (TPR) techniques. The catalytic performances of the prepared samples showed the best catalytic results for the catalyst which was prepared by the co-impregnation of In, Sn and Fe in the first step followed by Pt and Li impregnation in the second and third step, respectively. The synthesized support also performed well as an efficient carrier for the dehydrogenation catalyst of higher normal paraffins.

Key words: Nanomaterials, sol–gel preparation, γ-Al_2O_3, dehydrogenation catalyst, catalyst modifiers, successive impregnation.

INTRODUCTION

Dehydrogenation of hydrocarbons is an important commercial process because of the great and expanding demand for dehydrogenated hydrocarbons for use in the manufacture of various chemical products (Bell, 1992). All the dehydrogenation catalysts of long chain paraffins are designed to produce linear olefins for the manufacture of biodegradable detergents from raw materials such as C_{10} to C_{13}, C_{11} to C_{14}, C_{11} to C_{15}, and mixtures of the like (Padmavathi et al., 2005). Platinum and platinum-containing bimetallic catalysts supported on alumina are widely used for naphtha reforming and for heavy linear alkanes (C_{10}-C_{15}) dehydrogenation in the petrochemical industries. However, recently these kinds of catalysts have also been used for dehydrogenation of light paraffins. The difference between dehydrogenating and reforming catalysts relies mainly on the acidity of the support. Reactions catalyzed by the acidic sites of the support (such as isomerization, cracking and polymerization) must be inhibited in order to increase the yield to olefins in the dehydrogenation processes (Miguel et al., 1995; Pieck et al., 2005).

The key role of dehydrogenation catalysts is to accelerate the main reaction while controlling the other side reactions (Bhasin et al., 2001). In the case of dehydrogenation of long chain alkanes, a multimetallic alumina supported platinum catalyst is implemented, which contains In and Sn promoters as platinum modifiers, and alkaline and alkaline-earth metals as support modifiers. Promoters improve the activity, selectivity and stability of platinum–alumina catalysts (Gaidai et al., 2001;

*Correspondingauthor. E-mail: akia.mandana@gmail.com.

Gokak et al., 1996). Multicomponent oxides usually show higher activity, longer life time, and better resistance to poisons than the single-component oxide. The majority of multicomponent catalysts for the dehydrogenation of higher normal paraffins have been reported in patents (Dongara et al., 1997; Wilhelm, 1993).

The addition of Sn to Pt/Al_20_3 catalysts improves the activity and selectivity to olefins in the dehydrogenation reaction, while increasing the catalyst stability (Passes et al., 2000; Castro and Catal, 1993; Sanfilippo et al., 2006). Indium as a modifier decreases the hydrogenating capacity of alumina and suppresses olefin cracking and isomerization, probably as a result of a decrease in the acidic function of the support. The addition of Sn to Pt/Al_2O_3 catalysts has been investigated in several studies, while the effect of In received less attention (Passos et al., 1998). Incorporation of iron in this catalyst increases both the activity and the stability of the catalyst (Dongara et al., 1997). Studies the effect of impregnation sequences in dehydrogenation catalysts are mostly reported for bimetallic catalysts (Baronetti et al., 1985; Kappenstein et al., 1995).

Alumina is the most widely used support material for the dehydrogenation catalysts because of its superior capability to maintain a high degree of platinum dispersion which is essential for achieving high dehydrogenation activity.

But its strong acidity causes side reactions and coke formation (Bhasin et al., 2001). The addition of alkaline and alkaline-earth ions (for example, Li) to γ-Al_2O_3 selectively poisons the isomerization active sites, without affecting the dehydrogenation capacity of the catalytic systems (Siri et al., 2005). The sol-gel techniques have been widely applied for the synthesis of highly porous alumina which originally was developed by Yoldas (1975). The advantages of the sol-gel method includes the ability of maintaining high purity, changing the physical characteristics such as pore size distribution, pore volume and preparing samples at low temperatures (Farias et al., 2003; Zhang et al., 2002).

In this study high surface area nanocrystalline gamma alumina support was synthesized by the sol-gel method and employed as a catalyst carrier for n-dodecane dehydrogenation catalyst (Pt-based catalyst). The effects of different successive impregnation methods for Pt, Sn and In elements were investigated in normal dodecane dehydrogenation reaction.

EXPERIMENTAL

Materials

Aluminium isopropoxide, (AIP, 99 wt%), hexadecyl trimethyl-ammonium bromide (C_{16}TMABr, 99 wt%), and nitric acid were used for the synthesis of gamma alumina. Hexachloroplatinic acid (H_2PtCl_6), tin chloride ($SnCl_2$), indium chloride ($InCl_3$), hydrochloric acid (HCl), lithium nitrate ($LiNO_3$) and iron nitrate ($Fe(NO_3)_3$) were used as metal precursors for catalyst preparation. Normal dodecane and high purity hydrogen (99.99%) were used for the catalytic reactions.

Support preparation

Preparation of the nanocrystalline gamma alumina support based on the method which was described by Akia et al. (2009, 2010). In short, the aluminium isopropoxide and hexadecyltrimethyl ammonium bromide were first dissolved in water. The molar ratios of water to AIP and hexadecyltrimethyl ammonium bromide to AIP were chosen as 90 and 0.8, respectively. The hydrolysis step was carried out at a temperature of 80°C for a time period of 30 min, under vigorous stirring. Subsequently the mixture was peptized using nitric acid (10 wt%) under vigorous stirring by careful pH adjustment to 6.5. The mixture was aged at ambient temperature for 5 h. The condensation of the mixture resulted from the evaporation of the solvent by heating the reaction mixture and subsequent drying in an oven at 110°C for 15 h.

Finally, the dried sample was calcined at 550˚C for 5h in order to remove the surfactant and obtain the gamma crystallite phase.

Catalyst preparation

The dehydrogenation catalyst consists of a synthesized or conventional gamma alumina support containing 0.5 wt% platinum, 0.5 wt% of tin, 0.3 wt% of indium, 0.2 wt% Fe, 0.6 wt% of lithium and less than 0.1 wt% of chloride. The catalyst samples were prepared by the successive incipient-wetness impregnation technique. In all the catalysts Fe was impregnated in the first step and Li in the final step. In a typical preparation method, Sn, Pt and Fe were first co-impregnated by the incipient-wetness technique on the gamma alumina support in a solution containing $SnCl_2$, $H2PtCl_6$, $Fe(NO_3)_3$ and 10 wt% HCl. This mixture was aged at room temperature for 4 h under stirring conditions. It was subsequently dried at 80°C for 18 h in a vacuum oven and calcined at 540°C for 2 h in air atmosphere.

In the second step, the calcined sample was impregnated with an aqueous solution containing a mixture of $In(Cl)_3$ and 10 wt% HCl to obtain the desired content of indium. The aging and drying step were done in the same way as the first stage. In order to reduce the chloride content (that is, less than 0.1 wt%), which is responsible for the side reactions, wet calcination was performed at a specific atmosphere which was a mixture of air and water (50/50 molar ratio). The resultant sample was further calcined in air atmosphere at 500°C for 2 h. In the final step, the dehalogenated sample was impregnated with an aqueous solution of lithium $LiNO_3/HNO_3$, followed by drying and calcination under the same conditions as mentioned earlier.

The other catalysts were prepared with the same procedure with the changes in the impregnation sequences. The actual concentrations determined by ICP–AES analyses are in good agreement with the theoretical values.

Characterization

To examine the crystallinity of the prepared samples, powder x-ray diffraction (XRD) analysis was carried out with a MAC Science Co. M18XHF diffractometer using CuKα X-ray radiation (λ= 0.1540 nm). The surface area (BET), pore size distribution and pore volume were determined by nitrogen adsorption at -196°C using an automated gas adsorption analyzer (Tristar 3000, Micromeritics). Scanning electron microscopy (SEM) was performed with HITACHI S-4800 FE-SEM operated at 5 Kv. Transmission electron microscopy (TEM) investigation was performed with JEOL JEM-2100UHR operated at 200 Kv. Temperature programmed reduction

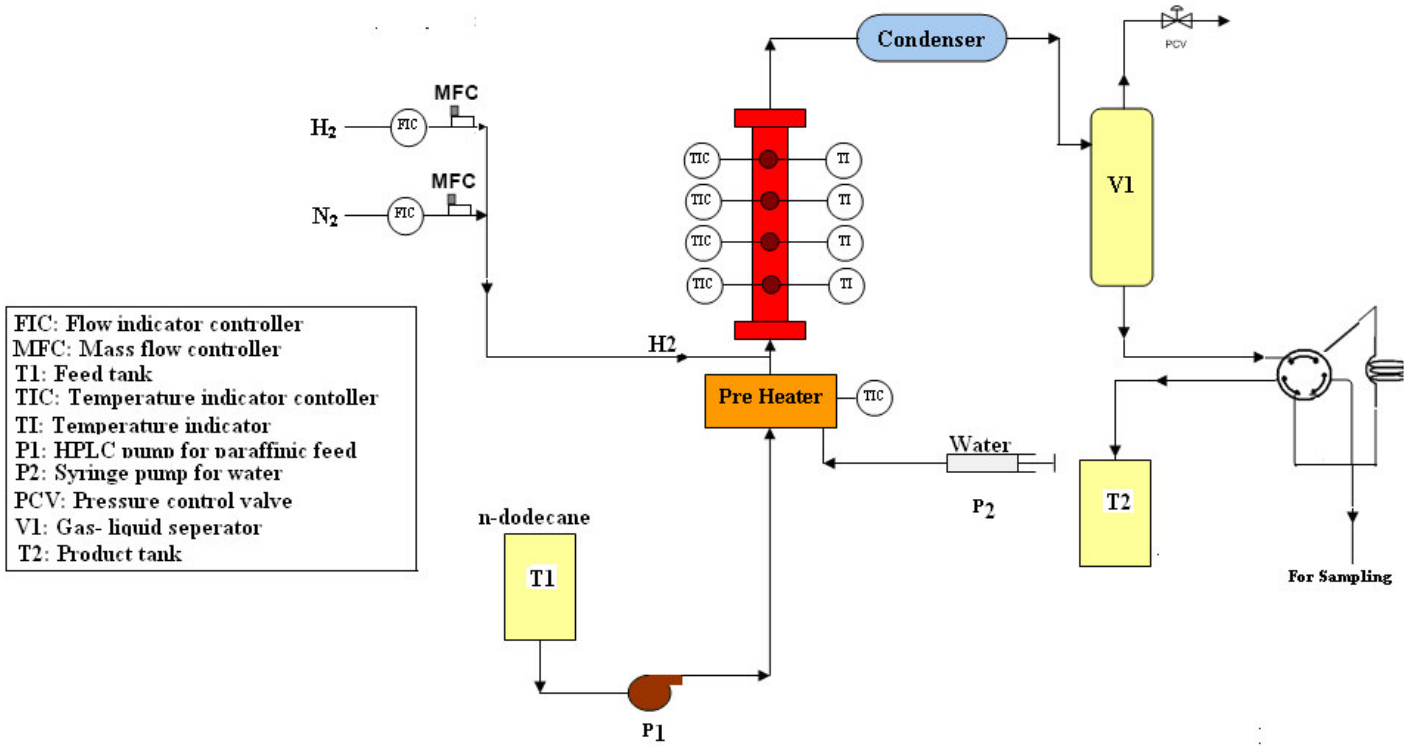

Figure 1. The schematic of the set- up for the dehydrogenation of normal dodecane paraffin.

Table 1. The operating parameters in the dehydrogenation of C_{12} paraffin.

Feed	Operating parameters	Reactor type
Normal paraffin C_{12} Hydrogen (99.99%)	Temperature: 460-490˚C. Pressure: 1-1.7 bar Liquid hourly space velocity (LHSV) of feed: 20 h–1, Hydrogen/hydrocarbon molar ratio: 6 Water: 2000 ppm wt%.	Up-flow fixed bed reactor.

(TPR) was carried out using an automatic apparatus (ChemBET-3000 Quantachrome) equipped with a thermal conductivity detector.

The fresh catalyst (500 mg) was subjected to a heat treatment (10℃/min) in a gas flow (50 ml/min) containing a mixture of H2:Ar (10:90). Before conducting the TPR experiment, the sample was heat treated under an inert atmosphere at 400 ˚C for 3 h.

Experimental set-up for catalyst evaluation

The schematic diagram of the experimental set-up used for the catalyst evaluation is shown in Figure 1. Major sections in the unit are: (1) Hydrogen flow control module, (2) Liquid pumping system, (3) Syringe pump for water, (4) Preheater and mixer for hydrogen, feed and water, (5) Reactor, (6) Condenser and gas–liquid separator, (7) Adequate flow meters to account material balance. The reactor is a tubular fixed-bed type with an inner diameter of 1.9 cm which is operated in isothermal and up-flow mode. Reactor internal temperature is measured with a central temperature probe with 4 thermocouples. Reactor inlet pressure is continuously monitored with a pressure transmitter.

Prior to the experiments all the catalysts, previously 20 to 40 mesh sieved were reduced under flowing H_2 at 430℃ for 4 h with a heating rate of 5℃/min. These catalysts were tested for 36 h on stream. The dehydrogenation reactions were carried out at three temperatures; 460, 475 and 490℃. The reactor effluent is cooled down in a water cooler and then enters the separator. Liquid analysis is performed on the product for analysis of the following components: Paraffins, olefins and diolefins, iso-paraffins, alkyl aromatics and alkyl naphthenes and cracked products. This is achieved with FID detector and HP PONA column.

Reaction conditions, which were the same for all the tests, are summarized in Table 1. As it can be seen in Table 1, hydrogen is utilized in amounts sufficient to ensure hydrogen to hydrocarbon mole ratio of about 6:1. Excess hydrogen is necessary in the dehydrogenation of lower and higher paraffins. Hydrogen serves a dual-function in both diluting the paraffin and suppressing the formation of hydrogen deficient, carbonaceous deposits on the catalyst composite.

When hydrogen is used as the diluent, a preferred practice is to add water or a water-producing compound to the dehydrogenation zone (Gaidai et al., 2001; Wilhelm, 1993).

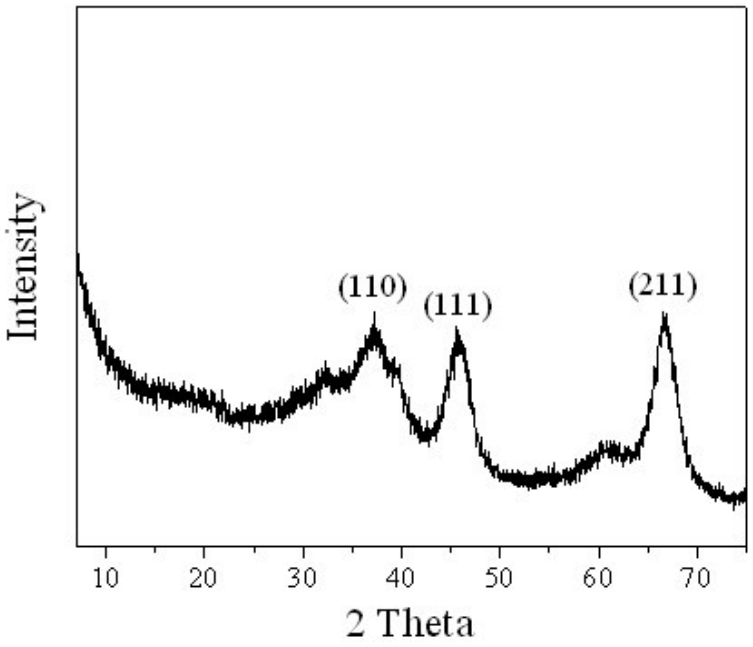

Figure 2. XRD pattern of the prepared Al_2O_3 calcined at 550°C.

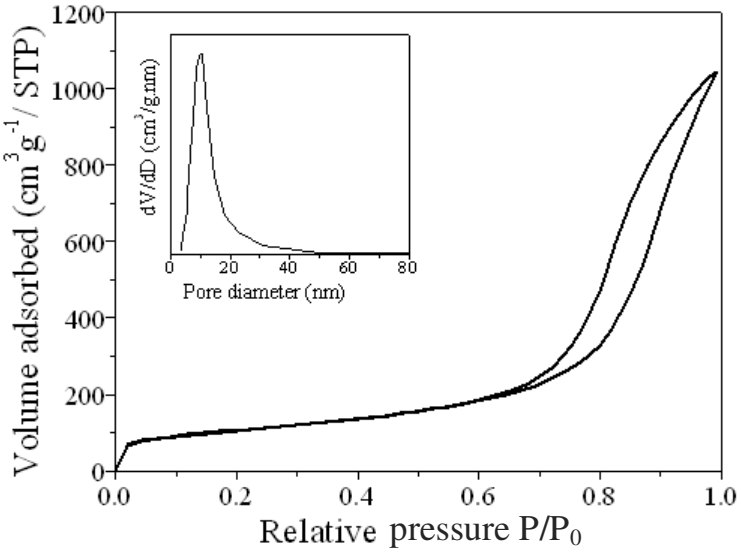

Figure 3. Nitrogen adsorption/desorption isotherm and pore size distribution (upper inset) of the Al_2O_3 calcined at 550°C.

RESULTS AND DISCUSSION

Texture and surface properties of γ-Al_2O_3

Aluminum alkoxide is hydrolyzed with water, producing aluminum mono- or trihydroxides. In both cases X-ray diffraction patterns of the initial products are the same. Poorly crystallized boehmite (pseudoboehmite) develops after a few hours while aging the precipitate. Boehmite is the only phase occurring if the temperature exceeds 77°C during the hydrolysis reaction or during aging of an initially amorphous precipitate (Dilsiz et al., 2002). The XRD pattern of the alumina sample calcined at 550°C is shown in Figure 2. As it can be seen, the sample is in the gamma crystallite phase.

The nitrogen adsorption/desorption isotherm and pore size distribution of the Al_2O_3 calcined at 550°C are shown in Figure 3. It can be concluded that the sample exhibits the classical shape of a type IV isotherm according to the IUPAC classification, typical for mesoporous solids

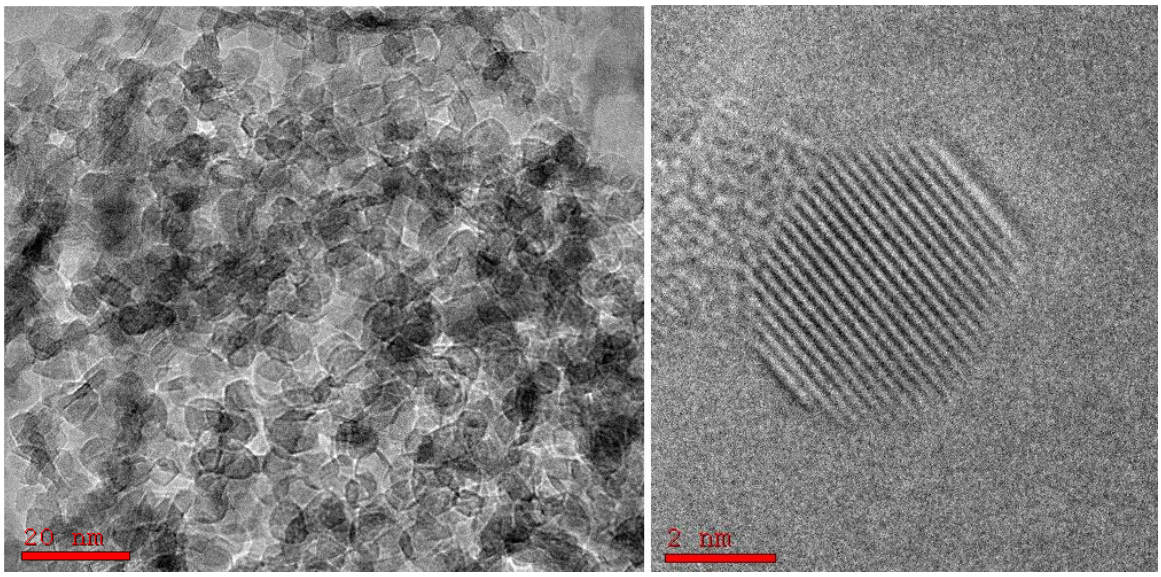

Figure 4. TEM images of the prepared γ -Al_2O_3 sample calcined at 550°C.

(Leofantia et al., 1998). However, for this sample, a hysteresis loop (type H1) occurs at a higher relative pressure range (p/p_0= 0.7 to 0.9) suggesting a broad pore size distribution with uniform size and shape. The pore size distribution (Figure 3, upper inset) indicates a meso-porous structure and also confirms a relatively broad pore size distribution. The BET surface area, average pore diameter and pore volume for the synthesized support were 328 m^2g^{-1}, 16.21 nm and 1.61 cm^3g^{-1}, respectively.

Figure 4 shows the TEM images of the synthesized gamma alumina. As it can be seen the prepared alumina highly crystallized with almost uniform size and/or shape particles. The TEM images indicate the presence of hexagonal crystal structure. The results also confirm the nanocrystallinity of the synthesized gamma alumina support (less than 4 nm).

Catalyst characterization and evaluation of catalytic performance

The results listed in Table 2 represent the different impregnation steps and the structural properties of the prepared catalysts. The BET results reported in Table 2 indicate that the catalysts for which platinum was impregnated in the first step had smaller pore volumes compared to other catalysts for which platinum was impregnated in the second step. The first step platinum impregnated catalysts also showed narrower pore size distributions in comparison to the other catalysts. The results indicate that the largest pore diameters (more than 6 nm) were obtained in catalysts for which platinum was impregnated in the second step. All the catalysts for which platinum was first impregnated had smaller pore diameters (less than 6 nm). Figure 5 shows the nitrogen adsorption isotherms at -196°C and the BJH pore size distributions (upper inset) of the two catalyst samples (2 and 7 as specified in Table 2) prepared with different impregnation sequences. The isotherms show the classical shape of the type IV according to the IUPAC classification, typical for mesoporous solids (Leofantia et al., 1998). However, for these samples, a hysteresis loop (type H3) occurs at lower relative pressures, suggesting a narrow pore size distribution. The pore size distributions (Figure 5, upper inset) confirm this assertion. Furthermore the pore size distribution for Cat. #7 shows a wider range in comparison to Cat. #2. It has been reported that alumina support with surface area higher than 150 $m^2\ g^{-1}$ shows good dispersion of metals.

Based on the research which investigated the effect of pore size on the platinum dispersion, it was revealed that dehydrogenation catalysts supported on alumina with small pores (more than 30% in the range of 2 to 10 nm) have dispersion more than 70% (Sharma et al., 2002). These results are also confirmed in (Merlen et al., 1996; Gomez et al., 1996; Bocanegra et al., 2006). The pore size distribution of all the prepared samples are mainly in the range from 2 to 10 nm, which means there is a good dispersion of platinum on the gamma alumina support with high surface area (328 m^2g^{-1}). Figure 6 represents the SEM image of Cat. #2 and Cat. #7. The surface image of Cat. #7 shows better distribution of the metals, but Cat. #2 indicates larger aggromerization of particles on the support.

Micrographs of transmission electron microscopy of Cat. #7 are shown in Figure 7. The dark spots in Figure 7(a) are believed to be metal clusters, while the lighter areas correspond to the gamma alumina support. In high resolution micrograph (Figure 7b), the Pt nanoparticles can be observed. Different catalysts prepared were

Table 2. The Textural properties of the dehydrogenation catalysts prepared with various impregnation sequences.

Catalyst #	Steps of impregnation	BET (m^2 g^{-1})	Pore diameter (nm)	Pore volume (cm^3g^{-1})
1	Pt+Sn+Fe – In – Li	179.03	4.35	0.25
2	Pt+Sn+In+Fe– Li	199.92	5.16	0.33
3	In+Fe– Pt+Sn – Li	187.87	6.03	0.47
4	Pt+Fe – In+Sn – Li	187.90	4.95	0.27
5	Sn +Fe – Pt+In– Li	217.69	6.76	0.51
6	Pt+Fe+In – Sn – Li	197.42	5.51	0.35
7	In+Sn+Fe – Pt – Li	227.74	6.41	0.51
8	In+Sn+Fe – Pt – Li	116.5	6.25	0.41

evaluated in the n-dodecane dehydrogenation reaction. Table 3 shows the catalytic performances of the samples at three different temperatures. The total conversion, olefin percentage and the selectivity for olefinic products are presented in Table 3. It is evident for all the samples, with an increase in temperature, the total conversion increased but the selectivity to olefinic products decreased because of the increase in the side reactions. The olefinic products which presented in Table 3 are mostly alfa monoolefins which is the desired product in higher normal paraffins dehydrogenation. In the samples 1, 2 and 3, platinum and tin co-impregnated. In sample 1, indium impregnated after them, in sample 2 indium co-impregnated and in sample 3, indium impregnated before them. As it can be observed, Cat. #3 showed better catalytic performance in comparison to the Cat. #1 and Cat. #2. In the samples 2, 4 and 7, tin and indium co-impregnated. In sample 2, platinum also co-impregnated, in sample 4 platinum impregnated before them and in sample 7, platinum impregnated after them. The catalytic results showed better performance for Cat. #7 in comparison to the Cat. # 2 and Cat. #4. In samples 2, 5 and 6, platinum and indium co-impregnated. In sample 2, tin co-impregnated with the other mentioned elements. In sample 5, tin impregnated before them and in sample 6, tin impregnated after them. Cat. #6 showed better catalytic results in comparison to the Cat. #2 and Cat. #5.

The results presented in Tables 2 and 3 indicate that the catalysts with smaller pore sizes and pore volumes also show good catalytic performances. The critical dimension for spherical molecules, computed by using the Lennard–Jones potential, was 1.24 (nm) for n-dodecane (Cruz et al., 2004). The results obtained in Table 2 showed that the pore volumes and pore diameters for the prepared catalysts were high enough for this reaction. But it must be noted that the large pores can minimize diffusion resistance. Sufficiently large pores are required for diffusion as the catalyst ages and fouls.

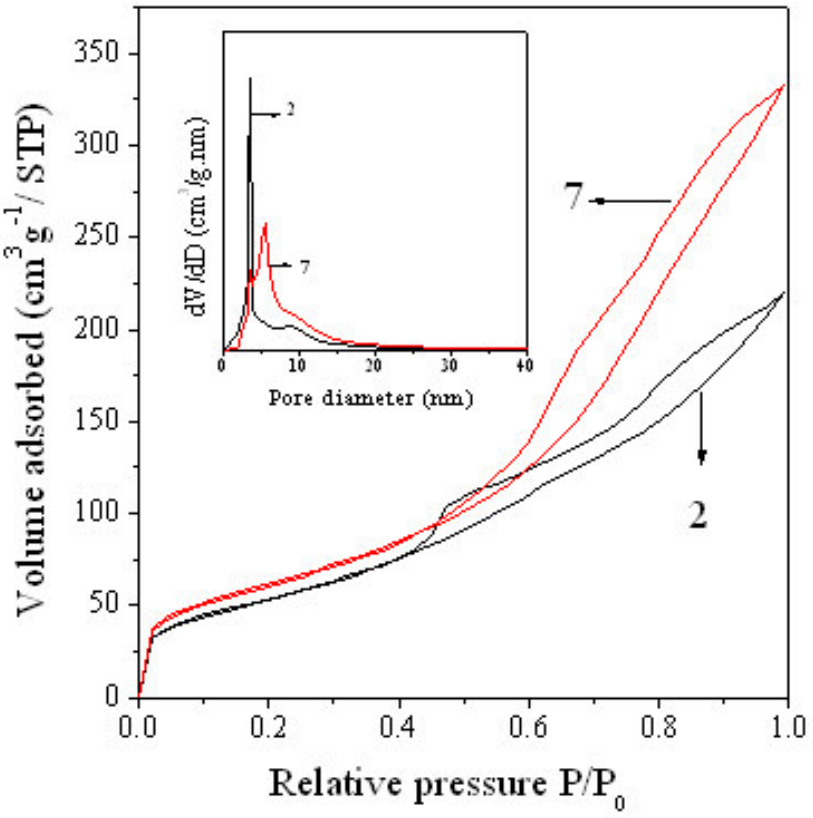

Figure 5. Nitrogen adsorption/desorption isotherm and pore size distribution (upper inset) of Cat. #2 and Cat. #7 prepared with different impregnation sequences.

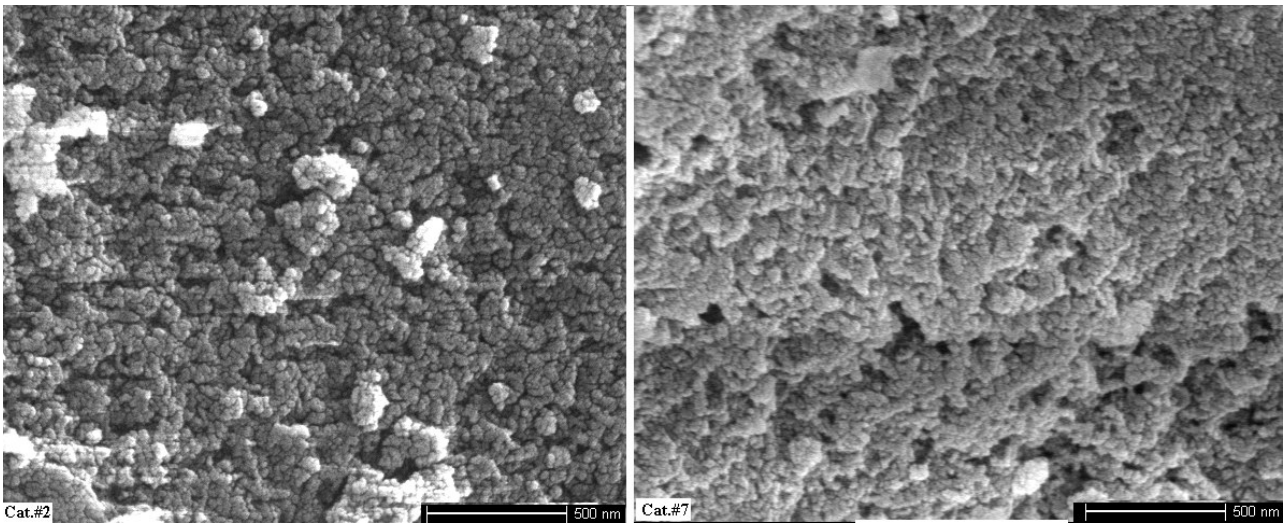

Figure 6. Micrographs of scanning electron microscopy of Cat. #2 and Cat. #7.

Our experimental results indicate that the catalyst which was prepared by co-impregnation of indium, tin and iron in the first step, impregnation of platinum in the second step, followed by lithium impregnation in the third step (Cat. #7), showed the best catalytic performance. The pore volume and the pore diameter for this sample were almost the highest among the other catalysts and the BET surface area was also the highest among the samples prepared. The results clearly showed the lower catalytic activity for the sample, which was prepared by

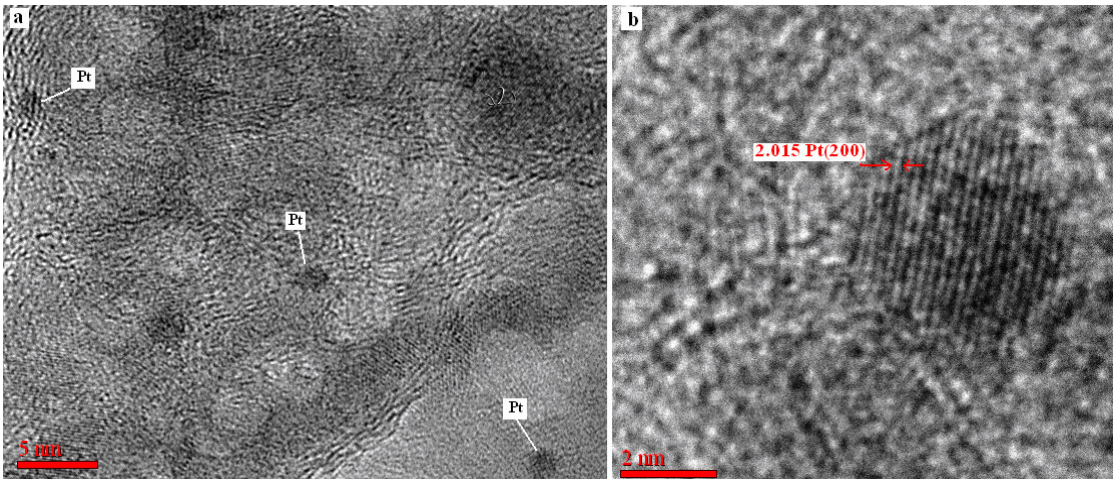

Figure 7. (a) Transmission electron micrograph and (b) high-resolution image of a Pt particle in Cat. #7.

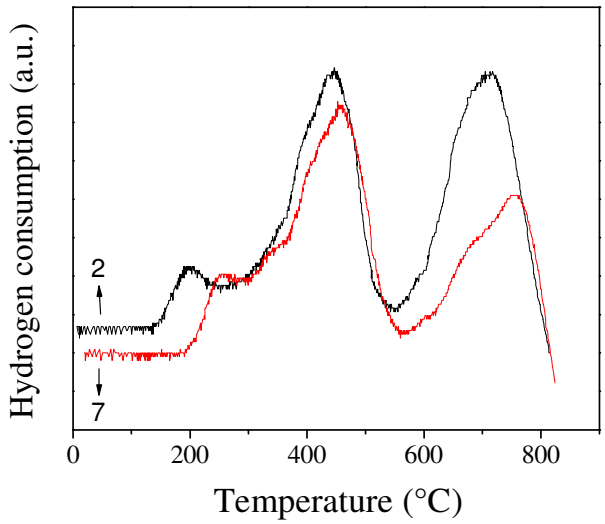

Figure 8. TPR profiles of two dehydrogenation catalysts (Cat. #2 and Cat. #7) prepared with the changes in the impregnation sequences.

co-impregnation of all the metals except lithium in the first step (Cat. #2).

The Cat. #8 was prepared with the conventional gamma alumina support to compare the effect of support on the performance of the dehydrogenation catalyst. The specific surface area, pore diameter and pore volume of the conventional gamma alumina support were 190 m^2 g^{-1}, 10 nm and 0.5 cm^3 g^{-1}, respectively. This catalyst was prepared with the impregnation sequences used for the Cat. #7. As it can be seen in Table 3, the catalytic results revealed that the synthesized support performed well as a good support to be used in dehydrogenation catalysts.

The TPR results for two catalyst samples (Cat. #2 and 7) are presented in Figure 8. For both catalysts, three main reduction zones appeared in the 150 to 320°C, 320 to 550°C and 550 to 800°C. The first small peak is related to the reduction of large Pt oxide or oxychloride crystals weakly interacted with the support. The second sharp peak indicates the co-reduction of Pt with the other metals (Sn and In).

The results of catalytic testing indicate that the catalysts with the first peak at relatively higher temperatures showed better catalytic activity. The shift of the first peak to the higher temperatures indicates the co-reduction of Pt with the other metals (Sn and In), which suggests a strong interaction between the metals with probable alloy formation. The alloys formation may break larger Pt ensembles into more finely distributed Pt species and thus improve the dispersion indirectly. As it was seen in Table 3, the highest and lowest catalytic

Table 3. The catalytic testing results of the prepared samples in the dehydrogenation reaction of n-dodecane at three different temperatures.

Catalyst #	Temp. (°C)	Total conversion (%)	Monoolefins (%)	Selectivity (%)
	460	9.06	7.08	78.20
1	475	11.75	8.03	68.37
	490	14.65	8.10	55.35
	460	6.70	5.00	74.76
2	475	8.88	4.66	52.49
	490	11.66	5.26	45.12
	460	10.08	7.58	75.2
3	475	13.2	8.59	65.07
	490	18.04	9.38	52.01
	460	8.64	6.92	80.13
4	475	12.27	8.84	72.08
	490	17.47	9.96	57.02
	460	11.14	8.00	71.8
5	475	12.93	8.47	65.46
	490	16.73	9.92	59.3
	460	10.23	8.04	78.572
6	475	12.75	9.45	74.15
	490	17.40	11.29	64.91
	460	11.39	8.80	77.31
7	475	14.03	10.18	72.55
	490	18.21	11.58	63.58
	460	10.18	7.23	71.04
8	475	12.86	8.38	65.2
	490	15.42	8.94	58.60

activity obtained for Cat. #7 and Cat. #2, respectively. As it is shown in Figure 8, the first reduction temperature for sample 7 was shifted to the higher temperatures in comparison to sample 2. This result also indicates the good interaction between active phase and its modifiers and consequently fine distribution of the platinum in Cat. #7. The TPR results for all the catalysts showed a reduction peak centered around 700°C, which is related to some portions of the oxides might be strongly bonded among themselves or with the support.

CONCLUSIONS

In this study high surface area nanocrystalline gamma alumina was prepared by the sol-gel method. The synthesized support was used as a carrier for dehydrogenation catalysts of higher normal paraffins. Different dehydrogenation catalysts were prepared with changes in the impregnation sequences of active phase (Pt) and its modifiers (Sn and In). It was observed that different impregnation methods lead to the different catalytic behaviors. The BET results revealed that smaller pore volumes were obtained for the catalysts which were impregnated with platinum in the first step. Based on the computed molecular size of n-dodecane, the results indicated that the pore sizes and pore volumes of all the catalysts were suitable for this reaction. But a higher pore catalyst improves accessibility of the hydrocarbons and reduces the possibility of the pores being plugged due to coke or metals deposition.

The best performance was obtained by Cat. #7, for which Fe, Sn and In were first impregnated, with Pt impregnation in the next step, followed by Li impregnation in the final step. The surface area, pore size and pore volume of Cat. #7 was almost the highest among the

catalysts prepared. The catalytic results also confirmed the ability of the synthesized nanocrystalline gamma alumina as a promising support for dehydrogenation catalysts of higher normal paraffins.

ACKNOWLEDGEMENTS

The authors acknowledge financial assistance of Research and Technology center of the petrochemical company in Iran.

REFERENCES

Akia M, Alavi SM, Rezaei M, Zi- Feng Y (2009). Optimizing the sol–gel parameters on the synthesis of mesostructure nanocrystalline γ-Al_2O_3. Microporous Mesoporous Mater., 122: 72

Akia M, Alavi S M, Rezaei M, Zi- Feng Y (2010 Synthesis of high surface area γ- Al2O3 as an efficient catalyst support for dehydrogenation of n-dodecane. J. Porous Mater., 17: 85

Baronetti GT, Miguel SR, Scelza OA, Fritzler A (1985). Pt-Sn/Al_2O_3 catalysts: studies of the impregnation step. Castro AA Appl C, 19: 77

Bell AT (1992). Catalysis Looks to the Future: National Academy Press, Washington D.C, p. 1992. 23.

Bhasin MM, McCain JH, Vora B V, Imai T, Pujado PR (2001). Dehydrogenation and oxydehydrogenation of paraffins to olefins. Appl Catal. A., 221: 397

Bocanegra SA, Castro AA, Ruız AG, Scelza OA, Miguel SRD (2006). Characteristics of the metallic phase of Pt/Al_2O_3 and Na-doped Pt/Al_2O_3 catalysts for light paraffins dehydrogenation. Chem. Eng. J., 118: 161

Castro AA (1993). Catalysts for the selective dehydrogenation of high molecular weight paraffins. Catal. Lett., 22: 123.

Cruz FJ, Laredo GC, (2004). Molecular size evaluation of linear and branched paraffins from the gasoline pool by DFT quantum chemical calculations. Fuel, 83: 2183.

Dilsiz N, Akoval G (2002). Study of sol–gel processing for fabrication of low density alumina microspheres. Mater. Sci. Eng., 332: 91

Dongara R, Basrur AG, Gokak DT, Gokak K V, Rao V, Krishnamurthy K R, Bhardwaj IS (1997 Catalyst composite for dehydrogenation of paraffins to mono-olefins and method for the preparation thereof. Bhardwaj I S US 5 677 260. 1997

Farias RF, Arnold U, Martinez L, Schuchardt U, Jannini MJDM, Airoldi C (2003). Synthesis, Characterization and Catalytic Properties of Sol-Gel Derived Mixed Oxides. J. Phys. Chem. Solids, 64: 2385

Gaidai N A, Kiperman S L, Kinet C (2001). Kinetic Models of Catalyst Deactivation in Paraffin Dehydrogenation Kinet Catal., 42: 527

Gokak DT, Basrur AG, Rajeswar D, Rao GS, Krishnamurthy KR (1996). Lithium promoted Pt/Sn/Al_2O_3 catalysts for dehydrogenation of n-decane: Influence of lithium metal precursor. React. Kinet. Catal. L, , 59: 315

Gomez R, Bertin V, Lopez T, Schifter I, Ferrat G (1996). Pt-Sn/Al_2O_3 sol-gel catalysts: catalytic properties. J. Mol. Catal. A. Chem., pp. 109: 55

Kappenstein C, Saouabe M, Guerin M, Marecot P (1995). Characterization and activity of Pt-Sn/Al_2O_3 catalysts of different preparation: coimpregnation and new Pt-Sn precursor. Catal J., 31: 9

Leofantia G, Padovan M, Tozzola G, Venturelli B, (1998). Surface area and pore texture of catalysts. Catal Today, 1998, 41: 207

Merlen E, Beccat P, Bertolini JC, Delichere P, Zanier N, Didillon B (1996). Characterization of Bimetallic Pt–Sn/Al_2O_3 Catalysts: Relationship between Particle Size and Structure. J Catal., 159: 178

Miguel S R, Castro A A, Scelza O A (1995). Catal Lett. Effect of the addition of alkali metals on the metallic phase of Pt/Al_2O_3 catalysts.Catal Lett., 32: 281

Padmavathi G, Chaudhuri K K, Rajeshwer D, Rao GS, Krishnamurthy KR, Trivedi PC, Hathi K K, Subramanyam N, Chem Eng Sci, (2005). Kinetics of n-dodecane dehydrogenation on promoted platinum catalyst. Chem. Eng. Sci., 60: 4119.

Passes FB, Andera DAG, Schmal M (2000 The state of Tin on Pt–Sn/Nb2O5 catalysts. Catal. Today, 57: 283

Passos FB, Andera DAG, Schmal M (1998). Characterization and Catalytic Activity of Bimetallic Pt-In/Al_2O_3 and Pt-Sn/Al_2O_3 Catalysts Catal J., 178: 478

Pieck CL, Vera CR, Querini CA, Parera JM (2005). Differences in coke burning-off from Pt–Sn/Al_2O_3 catalyst with oxygen or ozone. Appl. Catal. A., 278: 173

Sanfilippo D, Miracca I (2006). Dehydrogenation of paraffins: synergies between catalyst design and reactor engineering. Catal Today, 111: 133

Sharma LD, Kumar M, Saxena AK, Chand M, Gupta JK (2002). Influence of pore size distribution on Pt dispersion in Pt-Sn/Al_2O_3 reforming catalyst. J. Mol. Catal A. Chem., 185: 135

Siri GJ, Ramallo-Lopez JM, Casella ML, Fierro JLG, Requejo FG, Ferretti OA (2005). XPS and EXAFS study of supported PtSn catalysts obtained by surface organometallic chemistry on metals Application to the isobutane dehydrogenation. Appl. Catal. A, 278: 239

Wilhelm FC (1993). Dehydrogenation of hydrocarbons with a multimetallic catalytic composite. US 3 998 900. 1993

Yoldas BE (1975). Alumina sol-preparation from alkoxides. Am. Ceram. Soc. Bull., 54: 289.

Zhang Z, Hicks RW, Pauly TR, Pinnavaia TJ (2002). Mesostructured forms of gamma- Al2O3. J. Am. Chem. Soc., 124: 1592